Microstructural and morphological characterizations of nanocrystalline Ni–Cu–Fe thin films electrodeposited from electrolytes with different Fe ion concentrations

Umut Sarac · M. Celalettin Baykul

Abstract In the current study, ternary Ni–Cu–Fe thin films have been grown from the electrolytes with different Fe ion concentrations onto indium tin oxide coated glass substrates by galvanostatic electrodeposition at ambient temperature. The microstructural, compositional, and morphological properties have been characterized with respect to Fe ion concentration using X-ray diffraction (XRD), energy dispersive X-ray (EDX) spectroscopy, scanning electron microscopy (SEM), and atomic force microscopy (AFM). EDX results indicated that the Fe content within the films increased and Ni and Cu contents decreased as the Fe ion concentration in the electrolyte was increased. From the XRD analysis, it was observed that the films have two separate, Cu-rich and Ni-rich phases. It was also observed that the phase separation becomes weaker with increasing Fe ion concentration. All of the films have face-centered cubic structure and [111] preferred crystallographic orientation. The texture degree of the Ni-rich (111) phase increased with the Fe ion concentration. SEM and AFM measurements revealed that the surface morphology is considerably affected by the Fe ion concentration. The size of the grains formed on the film surface and the surface roughness decreased as the Fe ion concentration within the electrolyte increased.

U. Sarac (✉)
Department of Elementary Education, Bartın University, Bartın 74100, Turkey
e-mail: usarac428@hotmail.com

M. C. Baykul
Department of Physics, Eskişehir Osmangazi University, Eskisehir 26480, Turkey

1 Introduction

Magnetic thin films including iron group metals (Ni, Co, and Fe) grown by electrodeposition are important magnetic materials because of their potential applications in computer read/write heads and micro electrical mechanical system (MEMS) [1]. Among them, Ni–Cu–Fe system is known as one of the promising alternatives for sensors and magnetic recording medias industry [2]. Magnetic thin films can be produced by several deposition methods. Among them, electrodeposition or electrochemical deposition method has many unique advantages such as simplicity, less time-consuming, cost-effectiveness, and easy control of electroplating parameters and also it can be performed without high temperature and pressure [3–9].

In the present investigation, we have preferred to use the indium tin oxide (ITO) coated glass substrates for the preparation of the ternary Ni–Cu–Fe thin films by electrodeposition. Because ITO coated glass is an excellent transparent, conductive substrate and almost non–sensitive to external air and humidity, which make it a very suitable substrate in various experimental environments [10–13]. On the other hand, although ITO coated glass substrates have been frequently used for the deposition of semiconductor thin films, metallic Ni [12–19], Ni–Fe [20], Ni–Co [21], Fe–Co [22], Fe–Cu [23–25], and Ni–Cu [26–29] thin films have been also successfully electrodeposited onto ITO substrates in previous studies.

Electrodeposited film properties can be controlled by adjusting the growth parameters such as electrolyte composition, electrolyte pH, cathode potential, electrolyte temperature, and film thickness, etc. Particularly, the composition of the electrolyte used for the preparation of the deposits strongly affects the microstructural and morphological properties of electrodeposited thin films grown

onto ITO substrates [20–23]. To achieve the desired structural and morphological properties requires a detailed study on the evolution of microstructure and surface morphology. In this current study, therefore, the effect of Fe ion concentration in the electrolyte on the chemical compositions, microstructural, and morphological properties of the Ni–Cu–Fe thin films, which were electrodeposited onto ITO coated glass substrates at a constant current density of -15 mA/cm^2, were examined. The results obtained in this present work revealed that the Fe ion concentration in the electrolyte plays an important role on the microstructural properties and morphologies of the ternary Ni–Cu–Fe thin films.

2 Experimental details

Electrodeposited ternary Ni–Cu–Fe thin films were grown from the electrolytes having 0.07 M Ni sulfate, 0.01 M Cu sulfate, 0.05 M boric acid and Fe sulfate with different concentrations at a constant current density of -15 mA/cm^2. The Fe ion concentrations in the electrolyte were 0.005, 0.007, and 0.009. It must be mentioned here, Ni–Cu–Fe films were also electrodeposited at the Fe ion concentration of 0.011 M. However, Ni–Cu–Fe films could not be produced at this Fe ion concentration under these experimental conditions due to the brittle properties of the films. Deionized water was used to prepare all of the electrolytes. Electrolytes used for the electrodeposition of the films were freshly prepared before each experiment. Electrolyte pH value and temperature were 4.0 ± 0.1 and 25 ± 1 °C, respectively. All electrochemical depositions were carried out in a conventional three-electrode cell using a potentiostat/galvanostat (VersaSTAT 3). The working electrode was ITO substrate. The area of the substrates was about 0.8 mm^2. A platinum wire was used as a counter electrode and a saturated calomel electrode was employed as the reference electrode. The substrate surfaces were cleaned in the medium for 5 min in acetone, 5 min in ethanol and finally rinsed with distilled water for 10 min prior to deposition process. Electrodeposition of the films was carried out at ambient temperature and pressure without stirring. Ni–Cu–Fe films were electrodeposited at a constant current density (-15 mA/cm^2) and the thicknesses of them were set around 0.8 μm for all electroplating conditions.

To study the structural properties of the films, X-ray diffraction (XRD) measurements were performed with a Panalytical-Empyrean XRD diffractometer (Cu K$_\alpha$ radiation, $\lambda = 0, 154,059$ nm) by scanning in the $2\theta = 40°–54°$ range with 0.05° steps. The morphological study of the films was performed using an atomic force microscopy (AFM) (Veeco, Multimode 5) in tapping mode operation
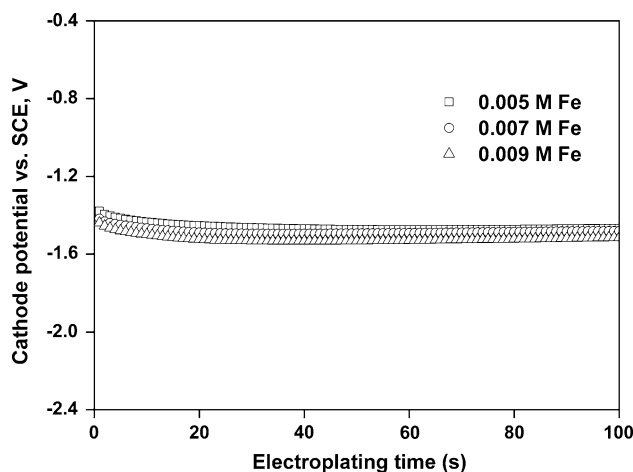

Fig. 1 Galvanostatic potential-time transients for ternary Ni–Cu–Fe thin film electrodeposition with respect to Fe ion concentration

and a scanning electron microscopy (SEM) (Zeiss Supra 40Vp). At the same time, the chemical compositional analysis of the films was achieved by the energy dispersive X-ray (EDX) facility of the SEM.

3 Results and discussion

In the present investigation, the effect of Fe content on the surface morphologies and microstructures of the Ni–Cu–Fe ternary thin films was examined by varying Fe ion concentration in the electrolyte. Initially, the galvanostatic potential-time transients of the films were recorded during deposition process in order to investigate the growth process. Figure 1 shows the galvanostatic potential-time transients recorded for the first 100 s of deposition process for the samples prepared from the electrolytes with different Fe ion concentrations. As seen from Fig. 1, the proper films are deposited since the cathode potentials are almost stable for all deposition conditions performed at different Fe ion concentrations. On the other hand, the cathode potential slightly decreases towards more negative values with increasing Fe ion concentration in the electrolyte.

The surface morphologies of the films were investigated using a SEM. The results of SEM analysis for the films electrodeposited from the electrolytes with 0.005 and 0.009 M Fe ion concentrations are shown in Fig. 2a, b, respectively. It is clearly seen that the surface morphology is considerably affected by the Fe ion concentration in the electrolyte. The surface of the films exhibits a morphology having of large cauliflower-like structures and small grains on the base part of the film irrespective of Fe ion concentration. In comparison to the film electrodeposited from
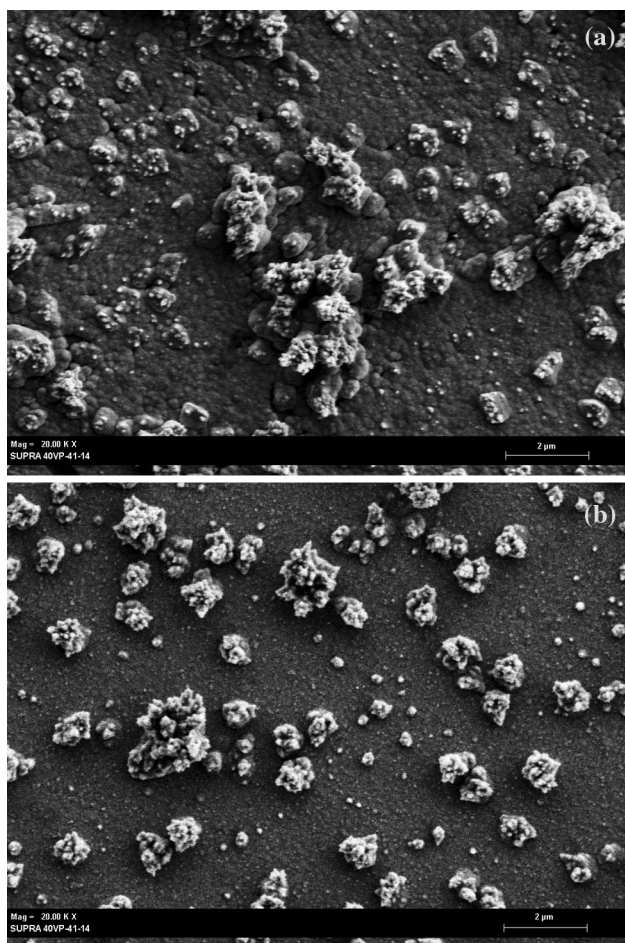
Fig. 2 SEM images of Ni–Cu–Fe thin films prepared from the electrolytes with different Fe ion concentrations **a** 0.005 M and **b** 0.009 M, respectively

Fig. 3 Composition of Ni–Cu–Fe thin films with the Fe ion concentration within the electrolyte

electrolyte with Fe ion concentration of 0.005 M (Fig. 2a), the SEM image of the film grown from electrolyte with Fe ion concentration of 0.009 M (Fig. 2b) shows that the size of the cauliflower-like structures decreases. The film surface exhibits more homogeneous and compact structure at high Fe ion concentration. A decrease in the size of cauliflower-like structures formed on the film surface with increasing Fe ion concentration contributes to the development of the smooth surface morphology. On the other hand, on the base part of the film, the size of grains also decreases and the number of them significantly increases with increasing Fe ion concentration.

The results of the compositional analysis performed by EDX over a large area of the films are summarized in Fig. 3. As shown from Fig. 3, the Fe content gradually increases from 5.4 to 11.2 at.% with increasing Fe ion concentration in the electrolyte from 0.005 to 0.009 M. However, the Ni and Cu contents within the deposits decrease over the range of the investigated Fe ion concentration. In addition, further EDX analysis also showed
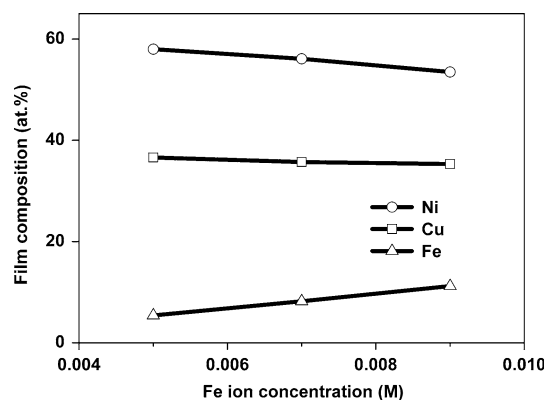
that the cauliflower-like structures include more Cu content than the base part of the films. The results obtained from the EDX measurements also reveal that the Ni–Cu–Fe films with different compositions exhibit anomalous behavior of two iron group elements (Fe and Ni). It is observed that the relative Fe concentration within the films is much higher than the relative ion concentration of Fe^{2+} in the electrolyte, indicating the anomalous codeposition. The anomalous codeposition has been also observed in electrodeposited NiFe films grown onto ITO coated glass substrates [20]. On the other hand, the relative Cu concentration within the films is much higher than the relative ion concentration of Cu^{2+} in the electrolyte.

XRD analyses were performed in order to investigate the crystallographic structure of the films. XRD measurements of the films were carried out on their substrates. Figure 4 shows the XRD patterns of the films prepared from the electrolytes with different Fe ion concentration and ITO coated glass substrate. XRD analyses reveal that all of the Ni–Cu–Fe thin films are polycrystalline. From the XRD patterns, the (111) and (200) diffraction peaks appeared at the angular positions of around 44° and 51°, respectively, which correspond to face-centered cubic (FCC) structure, are clearly seen. In all films electrodeposited at different Fe ion concentrations, reflections of body-centred cubic Fe phase are not observed from the XRD patterns since the films have low Fe content. However, the films have two segregated peaks at the angular position of around $2\theta = 44°$. One of them occurred at low angle can be ascribed to the (111) peak of FCC Cu-rich phase and the other one formed at high angle can be attributed to the (111) peak of FCC Ni-rich phase. It can be also clearly seen that the films have also two separate diffraction peaks at the angular position of around $2\theta = 51°$. The peak appeared at low angle corresponds to the (200) peak of FCC Cu-rich and the peak occurred at high angle corresponds to the (200) peak of FCC Ni-rich
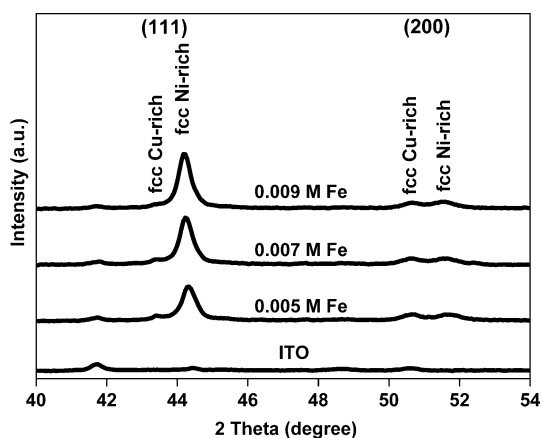
Fig. 4 XRD patterns of electrodeposited ternary Ni–Cu–Fe thin films grown from the electrolytes with different Fe ion concentrations

Fig. 6 Variation in normalized peak intensity depending on the Fe ion concentration within the electrolyte. All lines are guide for the eye
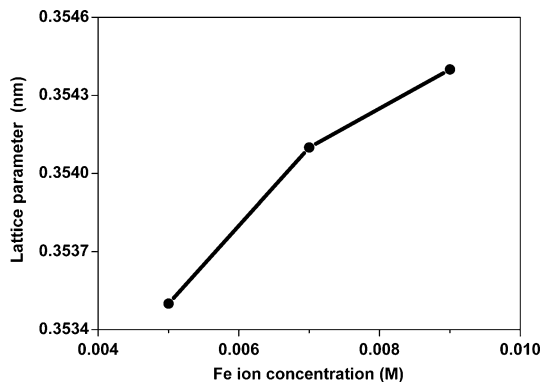

Fig. 5 The evolution of the lattice parameters in electrodeposited ternary Ni–Cu–Fe thin films with respect to Fe ion concentration within the electrolyte. All lines are guide for the eye

phase, respectively. These results show that the ternary Ni–Cu–Fe thin films exhibit a segregated Cu-rich and Ni-rich phases as observed in electrodeposited Ni–Cu systems [26–32].

Besides, the structural analysis also shows that the Ni-rich (111) peak position moves to lower 2θ angles as the Fe ion concentration in the electrolyte increases. We have calculated the lattice parameters of the Ni-rich (111) phase using the Bragg law from the XRD patterns with respect to Fe ion concentration in the electrolyte. The calculated lattice parameters of the Ni-rich (111) phase as a function of Fe ion concentration are shown in Fig. 5. The lattice parameter of the Ni-rich (111) phase increases as the Fe ion concentration in the electrolyte increases. This phenomenon might be attributed to the increase of the Fe content within the films. An enhancement of the lattice parameter with increasing Fe content in the FCC Ni–Fe films has been also reported [33, 34]. Also, there is a shift in the peak
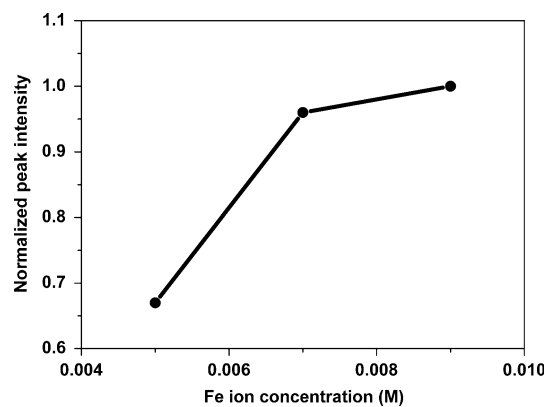
position of the Ni-rich (200) phase towards lower angle with increasing Fe ion concentration in the electrolyte, reflecting an increase in the lattice parameter of the Ni-rich (200) phase. The average crystallite size was determined from the full-width at half maximum value of the Ni-rich (111) peak using Scherrer formula [35]. They were found to be in the range of 19.5–21.3 nm, indicating that all of deposits obtained in the present work have fine nanosized crystallites.

On the other hand, the relative intensities of the (111) peak of the Ni-rich and Cu-rich phases are observed to change with the Fe ion concentration in the electrolyte (see Fig. 4). The relative intensity of the Ni-rich (111) diffraction peak increases as the Fe ion concentration in the electrolyte increases. However, the relative peak intensity of the Cu-rich (111) phase decreases with increasing Fe ion concentration in the electrolyte. This result may reflect that the phase separation becomes weaker with increasing Fe ion concentration in the electrolyte. Another possible contribution for the change of the morphological properties with Fe ion concentration may be this phase separation as observed from the XRD analysis. At the highest Fe ion concentration, the phase separation is weaker and this may contribute to the development of the smooth surface morphology as observed from the SEM measurements.

Besides, XRD intensity data is also used to estimate the relative crystalline degree of the Ni-rich phase as a function of Fe ion concentration in the electrolyte. The evolution of the normalized peak intensity as a function of Fe ion concentration in the electrolyte is given in Fig. 6. The value of peak intensity ratio was determined from the ratio of the peak intensity of Ni-rich (111) to that of the (200) one. All values shown in Fig. 6 were normalized such that the film with the highest peak intensity ratio has a value of 1. An increase in normalized peak intensity is due to the improvement in the crystalline degree of the Ni-rich (111)
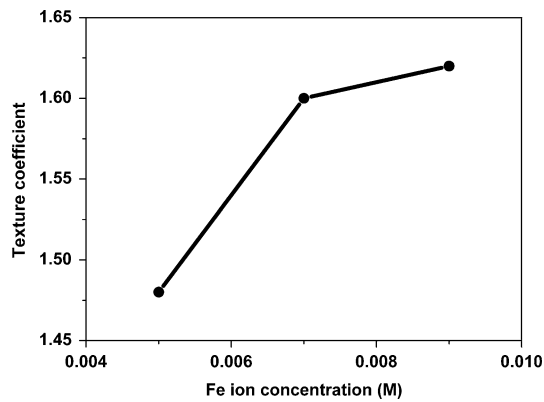
Fig. 7 The evolution of texture coefficients as a function of Fe ion concentration within the electrolyte. All lines are guide for the eye

phase with increasing Fe content within the films caused by the increase of Fe ion concentration in the electrolyte.

The effect of Fe ion concentration in the electrolyte on the preferred orientation and the texture degree of the electrodeposited Ni–Cu–Fe films was also studied by evaluating the texture coefficient. The texture coefficient values of the Ni-rich (111) phase were calculated using the formula as described below [36],

$$T_{c(hkl)} = \frac{I_{(hkl)}/I_{0(hkl)}}{(1/N)\left(\sum_N I_{(hkl)}/I_{0(hkl)}\right)}$$

where the texture coefficient of the (hkl) plane is given as $T_{c(hkl)}$, 'N' is the number of reflections taken into account. $I_{(hkl)}$ is the measured intensity of the (hkl) reflection of the XRD peak corresponding to (hkl) planes under analysis, $I_{o(hkl)}$ is the relative intensity of the (hkl) reflection of a randomly oriented FCC Cu (or Ni) sample. It is well known that the value $T_{c(hkl)} = 1$ represents a film with randomly oriented crystallites. The evolution of the $T_{c(111)}$ value with the Fe ion concentration is shown in Fig. 7. The texture coefficient is expected to be one for the film, which has randomly orientation crystallites. The texture coefficients found for the deposits prepared from the electrolytes with different Fe ion concentration reveal that the <111>texture develops preferentially in our electrodeposited ternary Ni–Cu–Fe films grown onto ITO coated glass substrates. That result found for our electrodeposited ternary Ni–Cu–Fe thin films agrees very well with that reported for electrodeposited NiFeCu/Cu films electrodeposited onto Ti substrates [37] and also Ni [12–15, 18] and Ni–Cu thin films [27–29] grown onto ITO coated glass substrates. From Fig. 7, it is also concluded that an increase in the Fe concentration within the electrolyte, consequently an increase in the Fe content within the films increases the <111> texture strength of the Ni-rich phase of the ternary Ni–Cu–Fe thin films.
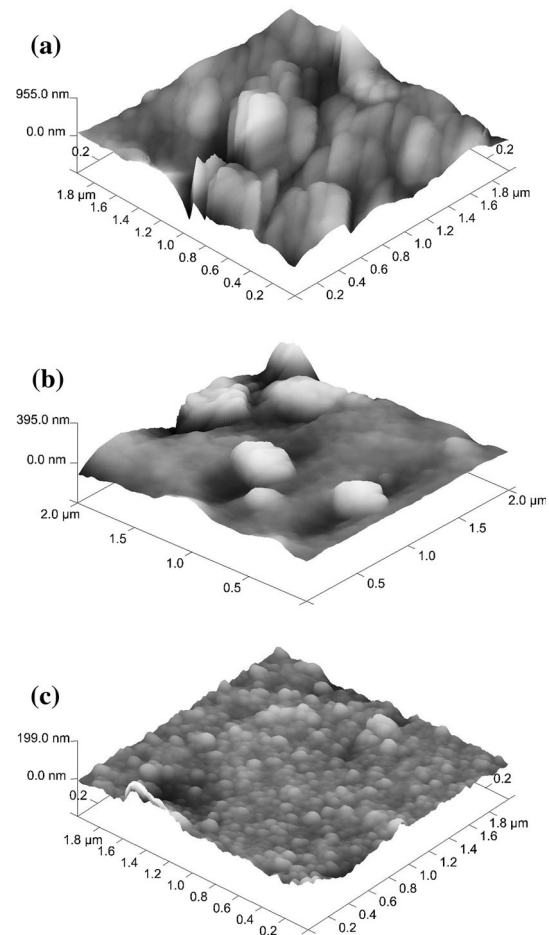

Fig. 8 Three dimensional AFM topographic images of Ni–Cu–Fe thin films electrodeposited from the electrolytes with different Fe ion concentrations **a** 0.005 M **b** 0.007 M, and **c** 0.009 M, respectively

In order to get a better understanding of the surface morphology, further investigation was performed by tapping mode AFM. Three-dimensional AFM images of the films are shown in Fig. 8. AFM images reveal that the surface of the films exhibits granular growth morphology regardless of Fe ion concentration. The results illustrated in Fig. 8 also show that the sizes of grains formed on the film surfaces decrease in both lateral and vertical directions, whereas the number density of them increases with increasing Fe ion concentration in the electrolyte. These results obtained from the AFM analysis are in good agreement with the SEM results. On the other hand, Fe ion concentration dependent change of the surface roughness of the films is shown in Fig. 9. As seen from Fig. 9, the surface roughness significantly decreases with increasing Fe ion concentration in the electrolyte. Moreover, if the variation of texture degree with the Fe ion concentration is considered (see Fig. 7), it can be clearly seen the presence of a direct correlation between the texture degree and surface roughness, i.e., the higher the texture degree the lower the surface roughness.
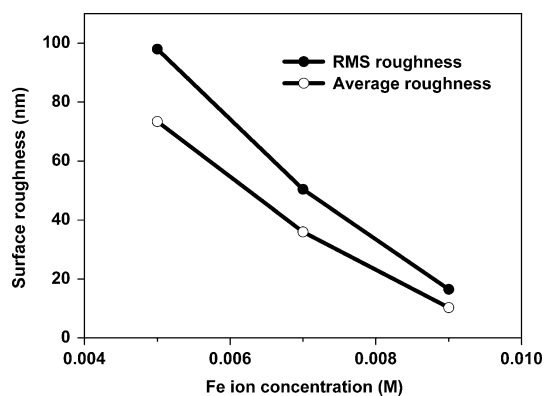
Fig. 9 Variation in average and RMS surface roughness of Ni–Cu–Fe thin films as a function of Fe ion concentration. All lines are guide for the eye

Accordingly, it is concluded that a variation in the Fe ion concentration within the electrolyte, hence the Fe content within the films has a strong influence on the surface morphologies and microstructural properties of the electrodeposited ternary Ni–Cu–Fe thin films prepared onto ITO coated glass substrates and the investigated properties of the films correlate very well with each other. Surface morphology has a significant role in various areas of science and technology [38]. Furthermore, the resistivity and magnetic properties of the films are affected by the surface roughness and microstructural properties of thin films [39–42]. Thus, the variations observed in the morphological and microstructural properties of the films in terms of Fe ion concentration within the electrolyte may provide beneficial information for possible applications of these deposits.

4 Conclusion

Nanostructured Ni–Cu–Fe thin films with different compositions were electrodeposited from the electrolytes containing different Fe ion concentrations. From the compositional analysis, it was observed that the Fe content within the films is consistent with the Fe ion concentration within the electrolytes. XRD studies revealed the existence of segregated Cu-rich and Ni-rich phases within the films. However, the phase separation was found to be weaker at higher Fe contents. Ni–Cu–Fe films investigated in the present study were found to have FCC structure and [111] preferred crystallographic orientation. However, the degree of the <111> texture of the Ni-rich (111) phase increased with increasing Fe content. From the SEM measurements, it was observed that the films exhibit a morphology consisting of large cauliflower-like structures and small grains on the base part of the films. All films investigated with

AFM were found to be covered with grains of varying size. The size of grains occurred on the film surface decreased while the number density of them increased as the Fe content within the films increased. The roughness values of the film surfaces improved as the Fe content within the films increased. A correlation between the surface roughness and texture degree was observed, i.e., the smaller the surface roughness the higher the texture degree. As a result, the study clearly showed that the Fe content provides an improvement in the microstructural and surface morphological properties of the electrodeposited ternary Ni–Cu–Fe thin films grown onto ITO coated glass substrates and the investigated properties of the films can be controlled via Fe ion concentration in the electrolyte.

References

1. D. Kim, D.Y. Park, B.Y. Yoo, P.T.A. Sumodjo, N.V. Myung, Electrochim. Acta **48**, 819 (2003)
2. I. Prioteasa, V. Ciupină, I.M. Oancea-Stănescu, G. Prodan, C. Ştefanov, Optoelectron. Adv. Mater.-Rapid. Commun. **6**, 597 (2012)
3. E. Pellicer, A. Varea, S. Pané, K.M. Sivaraman, B.J. Nelson, S. Suriñach, M.D. Baró, J. Sort, Surf. Coat. Technol. **205**, 5285 (2011)
4. J. Garcia-Torres, E. Gómez, E. Vallés, J. Electroanal. Chem. **635**, 63 (2009)
5. I. Bakonyi, L. Péter, Prog. Mater. Sci. **55**, 107 (2010)
6. I. Baskaran, T.S.N. Sankara Narayanan, A. Stephen, Mater. Lett. **60**, 1990 (2006)
7. S.K. Ghosh, A.K. Grover, G.K. Dey, M.K. Totlani, Surf. Coat. Technol. **126**, 48 (2000)
8. F.R. Bento, L.H. Mascaro, Surf. Coat. Technol. **201**, 1752 (2006)
9. Y.H. You, C.D. Gu, X.L. Wang, J.P. Tu, Surf. Coat. Technol. **206**, 3632 (2012)
10. J. Ebothe, J. Appl. Phys. **77**, 233 (1995)
11. P.R. i Cabarrocas, J.B. Chevrier, J. Huc, A. Lloret, J.Y. Parey, J.P.M. Schmitt, J. Vac. Sci. Technol. A **9**, 2331 (1991)
12. L. Nzoghe-Mendome, J. Ebothe, A. Aloufy, I.V. Kityk, J. Alloys Compd. **459**, 232 (2008)
13. L. Nzoghe-Mendome, A. Aloufy, J. Ebothé, D. Hui, M. El Messiry, Mater. Chem. Phys. **115**, 551 (2009)
14. L. Nzoghe-Mendome, A. Aloufy, J. Ebothé, M. El Messiry, D. Hui, J. Cryst. Growth **311**, 1206 (2009)
15. M. Saitou, A. Makabe, T. Tomoyose, Surf. Sci. **459**, L462 (2000)
16. M. Saitou, W. Oshikawa, A. Makabe, J. Phys. Chem. Solids **63**, 1685 (2002)
17. E. Gomez, R. Pollina, E. Vallés, J. Electroanal. Chem. **386**, 45 (1995)
18. S.Z. Chu, K. Wada, S. Inoue, S. Todoroki, Electrochim. Acta **48**, 3147 (2003)
19. M. Saitou, W. Oshikawa, M. Mori, A. Makabe, J. Electrochem. Soc. **148**, C780 (2001)

20. X. Su, C. Qiang, Bull. Mater. Sci. **35**, 183 (2012)
21. L. Tian, J. Xu, C. Qiang, Appl. Surf. Sci. **257**, 4689 (2011)
22. C. Qiang, J. Xu, S. Xiao, Y. Jiao, Z. Zhang, Y. Liu, L. Tian, Z. Zhou, Appl. Surf. Sci. **257**, 1371 (2010)
23. U. Sarac, M.C. Baykul, Adv. Mater. Sci. Eng. **2013**, 7 (2013)
24. U. Sarac, M.C. Baykul, J. Mater. Sci. Technol. **28**, 1004 (2012)
25. U. Sarac, M.C. Baykul, J. Mater. Sci. Mater. Electron. **24**, 952 (2013)
26. J.K. Chang, S.H. Hsu, I.W. Sun, W.T. Tsai, J. Phys. Chem. C **112**, 1371 (2008)
27. U. Sarac, R.M. Öksüzoğlu, M.C. Baykul, J. Mater. Sci. Mater. Electron. **23**, 2110 (2012)
28. U. Sarac, M.C. Baykul, J Alloy Compd. **552**, 195 (2013)
29. U. Sarac, M.C. Baykul, J. Mater. Sci. Mater. Electron. **24**, 2777 (2013)
30. L. Sun, C.L. Chien, P.C. Searson, Chem. Mater. **16**, 3125 (2004)
31. D.S. Kong, J.M. Wang, H.B. Shao, J.Q. Zhang, C.N. Cao, J. Alloys Comp. **509**, 5611 (2011)
32. M.J. Fesharaki, L. Peter, T. Schucknecht, D. Rafaja, J. Degi, L. Pogany, K. Neurohr, E. Szeles, G. Nabiyouni, I. Bakonyi, J. Electrochem. Soc. **159**, D162 (2012)
33. H. Li, F. Ebrahimi, Mater. Sci. Eng. A **347**, 93 (2003)
34. S.D. Leith, S. Ramli, D.T. Schwartz, J. Electrochem. Soc. **146**, 1431 (1999)
35. A.J.C. Wilson, Proc. Phys. Soc. Lond. **80**, 286 (1962)
36. S.A. Nasser, H.H. Afify, H.H. Afify, S.A. El–Hakim, Thin Solid Films **315**, 327 (1998)
37. M.C. Baykul, U. Sarac, M. Alper, J. Supercond. Nov. Magn. **25**, 2585 (2012)
38. J. Bałamucki, P. Czarnecki, T. Gotszalk, A. Marendziak, I. Rangelow, J. Wilk, Z.W. Kowalski, Phys. Chem. Solid State **7**, 577 (2006)
39. M. Li, Y.-P. Zhao, G.-C. Wang, H.-G. Min, J. Appl. Phys. **83**, 6287 (1998)
40. N.V. Myung, D.-Y. Park, B.-Y. Yoo, P.T.A. Sumodjo, J. Magn. Magn. Mater. **265**, 189 (2003)
41. S. Singh, S. Basu, Surf. Coat. Technol. **201**, 952 (2006)
42. R. Balachandran, H.K. Yow, B.H. Ong, K.B. Tan, K. Anuar, H.Y. Wong, Int. J. Electrochem. Sci. **6**, 3564 (2011)